Fine mapping of autophagy-related proteins during autophagosome formation in *Saccharomyces cerevisiae*

Kuninori Suzuki[1,*], Manami Akioka[2], Chika Kondo-Kakuta[2], Hayashi Yamamoto[2] and Yoshinori Ohsumi[2,*]

[1]Bioimaging Center, Graduate School of Frontier Sciences, University of Tokyo, FSB-101, 5-1-5 Kashiwanoha, Kashiwa, Chiba 277-8562, Japan
[2]Frontier Research Center, Tokyo Institute of Technology, 4259-S2-12 Nagatsuta-cho, Midori-ku, Yokohama, Kanagawa 226-8503, Japan
*Authors for correspondence (kuninori@k.u-tokyo.ac.jp; yohsumi@iri.titech.ac.jp)

Accepted 18 March 2013
Journal of Cell Science 126, 2534–2544

doi: 10.1242/jcs.122960

Summary

Autophagy is a bulk degradation system mediated by biogenesis of autophagosomes under starvation conditions. In *Saccharomyces cerevisiae*, a membrane sac called the isolation membrane (IM) is generated from the pre-autophagosomal structure (PAS); ultimately, the IM expands to become a mature autophagosome. Eighteen autophagy-related (Atg) proteins are engaged in autophagosome formation at the PAS. However, the cup-shaped IM was visualized just as a dot by fluorescence microscopy, posing a challenge to further understanding the detailed functions of Atg proteins during IM expansion. In this study, we visualized expanding IMs as cup-shaped structures using fluorescence microscopy by enlarging a selective cargo of autophagosomes, and finely mapped the localizations of Atg proteins. The PAS scaffold proteins (Atg13 and Atg17) and phosphatidylinositol 3-kinase complex I were localized to a position at the junction between the IM and the vacuolar membrane, termed the vacuole–IM contact site (VICS). By contrast, Atg1, Atg8 and the Atg16–Atg12–Atg5 complex were present at both the VICS and the cup-shaped IM. We designate this localization the 'IM' pattern. The Atg2–Atg18 complex and Atg9 localized to the edge of the IM, appearing as two or three dots, in close proximity to the endoplasmic reticulum exit sites. Thus, we designate these dots as the 'IM edge' pattern. These data suggest that Atg proteins play individual roles at spatially distinct locations during IM expansion. These findings will facilitate detailed investigations of the function of each Atg protein during autophagosome formation.

Key words: Autophagy, Autophagosome, Isolation membrane, Autophagy-related genes, *ATG*, Pre-autophagosomal structure, PAS, Aminopeptidase I, Ape1, Ape1 complex, Starvation, Rapamycin, Endoplasmic reticulum exit sites, ERES, Yeast, Vacuole-isolation membrane contact site, VICS

Introduction

Macroautophagy, hereafter called simply 'autophagy,' is a bulk degradation system widely conserved among eukaryotes from yeast to mammals. When eukaryotic cells are faced with nutrient starvation, they degrade cytoplasmic materials to obtain building blocks that help them adapt to severe environmental conditions. Currently, over 30 autophagy-related (*ATG*) genes have been identified as necessary for various types of autophagy in yeast. Among them, 18 *ATG* genes are essential for autophagosome formation upon starvation (Mizushima et al., 2011; Nakatogawa et al., 2009). These Atg proteins are involved in autophagosome formation as components of several discrete functional units, but their interrelationships are not yet well understood.

Identification of the pre-autophagosomal structure (PAS) was an important milestone in the identification of the functioning Atg proteins. Using fluorescence microscopy, the PAS was initially found as a juxtavacuolar dot of Atg5 and Atg8 (Suzuki et al., 2001). The PAS was detectable in some *atg* disruptants, implying that the PAS can be organized regardless of autophagosome formation (Suzuki et al., 2001). The PAS is assembled through hierarchical interactions between Atg proteins. Early in the pathway, the upstream factors Atg11 and Atg17 modulate PAS assembly under nutrient-rich and starvation conditions, respectively (Shintani and Klionsky, 2004; Suzuki et al., 2007). Atg17 is a component of the Atg1–Atg13–Atg17–Atg29–Atg31 complex, which is responsible for recruitment of downstream Atg proteins upon starvation (Kawamata et al., 2008). Atg9 is one of these downstream Atg proteins (Suzuki et al., 2007). Atg9 is a membrane protein that is integrated into Golgi-derived vesicles called Atg9 vesicles (Yamamoto et al., 2012). A few Atg9 vesicles are targeted to the PAS (Yamamoto et al., 2012), suggesting that lipids are components of the PAS. After the PAS is assembled, it acts to generate the isolation membrane (IM), which ultimately becomes a closed autophagosome (Baba et al., 1997).

Atg8, one of the most downstream Atg proteins, is localized to the PAS, the IM and the autophagosome, and is subsequently delivered to the vacuole (Kirisako et al., 1999; Suzuki et al., 2001). Thus, Atg8 is used as a marker for all of these autophagic structures. However, two technical issues have obstructed further progress: in *Saccharomyces cerevisiae*, the IM is not

Journal of Cell Science

distinguishable from the PAS because of the resolution limit of light microscopy; moreover, the PAS has not been detected by electron microscopy. Therefore, in order to investigate the function of each Atg protein it was crucial to develop a method for discriminating the IM and PAS by fluorescence microscopy.

In this study, using *Saccharomyces cerevisiae* cells, we visualized the IM as a cup-shaped structure using fluorescence microscopy by enlarging a selective cargo of autophagosomes. Using this method, we were able to finely map the localizations of Atg proteins during IM expansion.

Results

Giant Ape1 complex enables to visualize isolation membranes

Vacuolar aminopeptidase I (Ape1) is synthesized as a proform (prApe1), and assembles into the Ape1 complex, in the cytoplasm (Shintani et al., 2002). The Ape1 complex associates with α-mannosidase and Ty1 virus–like particles to form the Cvt (cytoplasm-to-vacuole targeting) complex (Lynch-Day and Klionsky, 2010; Shintani et al., 2002; Suzuki et al., 2011). The Cvt complex is selectively enclosed in Cvt vesicles under nutrient-rich conditions, and in autophagosomes during starvation (Baba et al., 1997). Core Atg proteins are responsible for the formation of Cvt vesicles and autophagosomes (Xie and Klionsky, 2007). These double-membrane-bound structures fuse with the vacuole, in which prApe1 is processed to mature Ape1 (mApe1) (Klionsky et al., 1992). When prApe1 is moderately overexpressed, prApe1 accumulates under nutrient-rich conditions, but matures to mApe1 when cells are starved (Geng et al., 2008), probably because autophagosomes (~500 nm in diameter) have a larger cargo capacity than Cvt vesicles (~150 nm in diameter).

When prApe1 was highly overexpressed from a multicopy plasmid (supplementary material Fig. S1A), the majority of Ape1 was detected as prApe1 even under autophagy-inducing conditions (supplementary material Fig. S1B). Thus, overexpression of prApe1 exceeds the capacity of autophagy, causing prApe1 to accumulate in the cytoplasm. We examined the localization of overexpressed prApe1 in RFP–prApe1-expressing cells, and found that prApe1 formed a large spherical structure in the cytoplasm that was detectable even by bright-field microscopy (arrows in Fig. 1A). The diameter of these structures was ~1.7 μm on average (Fig. 1B). In these cells, vacuolar lumens were hardly stained with RFP (asterisks in Fig. 1A). Presumably, once the Ape1 complex exceeds a critical size, it becomes too large to be enclosed in an autophagosome, and instead forms a large structure that remains in the cytoplasm. We call the enlarged Ape1 complex the 'giant Ape1 complex' (GAC), hereafter.

In cells containing a GAC (hereafter, GAC cells), membranous structures were frequently associated with the GAC and the vacuolar membrane (arrowheads in Fig. 1C,D). This localization prompted us to hypothesize that these membranous structures are related to the IM. Therefore, we examined the localization of GFP–Atg8 in GAC cells. By fluorescence microscopy, we found that a cup-shaped structure between the GAC and the vacuole is indeed labeled with GFP–Atg8 (Fig. 1E). We measured the fluorescence intensity across the GAC, and confirmed that GFP–Atg8 is localized along the surface of the GAC (Fig. 1F). These results show that the IM can be visualized in GAC cells by fluorescence microscopy.

We examined the dynamics of IMs by time-lapse fluorescence microscopy. In the cell shown in Fig. 1G, a dot of GFP–Atg8 emerged between the GAC and the vacuole (40-seconds panel), then elongated along the surface of the GAC. Eventually, the IM ceased to elongate at the maximum size persistently (320–440-seconds; supplementary material Movie 1). To determine whether such a paused IM was a dead-end structure or not, a cup-shaped IM was examined by time-lapse fluorescence microscopy (Fig. 1H). The IM (arrowhead) disappeared from the surface of a GAC, and a new dot emerged at another site between the vacuole and another GAC (double arrowhead). The GAC still remained outside the vacuole (arrow). These results indicate that the cup-shaped IM is long-lasting at the maximum size but can be broken down physiologically.

In wild-type cells, the dynamics of GFP–Atg8 are difficult to follow by fluorescence microscopy, because the PAS moves on the surface of the vacuolar membrane, and autophagosome formation is completed within 10 minutes (Geng et al., 2008). In GAC cells, the dynamics of IM expansion can be followed because the GAC is much less mobile because of its larger mass, and the IM remains for a longer period at its maximum size. Thus, we have established a method for visualizing the maximum length stationary IMs in GAC cells.

Lengths of the IMs reflect the magnitude of autophagy

To investigate how Atg proteins are involved in IM expansion, we measured the maximum length of GFP–Atg8-labeled structures, which are localized between the GAC and the vacuole, under the fluorescence microscope. In wild-type cells, the maximum length of the cup-shaped IMs was ~1.21 μm (Fig. 2A,B). GFP–Atg8 accumulated at the PAS in *atg1*Δ, *atg2*Δ and *atg18*Δ cells (Suzuki et al., 2007). In these cells, GFP–Atg8 was localized at the PAS as an elliptical spot (Fig. 2A). The major axis of this elliptical spot was much shorter than the IM length observed in wild-type cells (Fig. 2B), suggesting that the IM does not expand in these gene disruptants. We conclude that Atg1, Atg2 and Atg18 are required for IM expansion.

Atg1 is a protein kinase and its kinase activity is essential for autophagy (Kamada et al., 2000; Matsuura et al., 1997). We examined whether the kinase activity of Atg1 was crucial for IM expansion. We used *atg1*^{K54A} and *atg1*^{D211A} mutants, which are defective in autophagy due to decreased kinase activity (Kamada et al., 2000; Matsuura et al., 1997). The kinase activity of Atg1 can be estimated by immunoblot analysis; the slower-migrating band represents autophosphorylated Atg1 (Stephan et al., 2009). Phosphorylated Atg1 slightly decreased in *atg1*^{K54A} cells but was not detected in *atg1*^{D211A} cells (Fig. 2C), suggesting that Atg1 kinase activity remains in *atg1*^{K54A} cells but not in *atg1*^{D211A} cells. We measured the maximum length of the IM in these mutants and found that the IMs in *atg1*^{K54A} and *atg1*^{D211A} cells were shorter than those in wild-type cells and that those in *atg1*^{D211A} cells were shorter than those in *atg1*^{K54A} cells (Fig. 2B). This result indicates that the length of the IM correlates with Atg1 kinase activity. Next, we quantified the activity of bulk autophagy using an alkaline phosphatase assay (Noda et al., 1995). Autophagic activity partially persisted in *atg1*^{K54A} cells but was completely abrogated in *atg1*^{D211A} cells (Fig. 2D). Taken together, these results suggest that the magnitude of bulk autophagy can be estimated from the IM lengths in GAC cells. Probably, the kinase activity of Atg1 plays a crucial role in IM expansion.

Fine mapping of Atg proteins on the IMs

Among vacuolar protein sorting (Vps) proteins, which are involved in sorting of Prc1 (also known as carboxypeptidase Y;

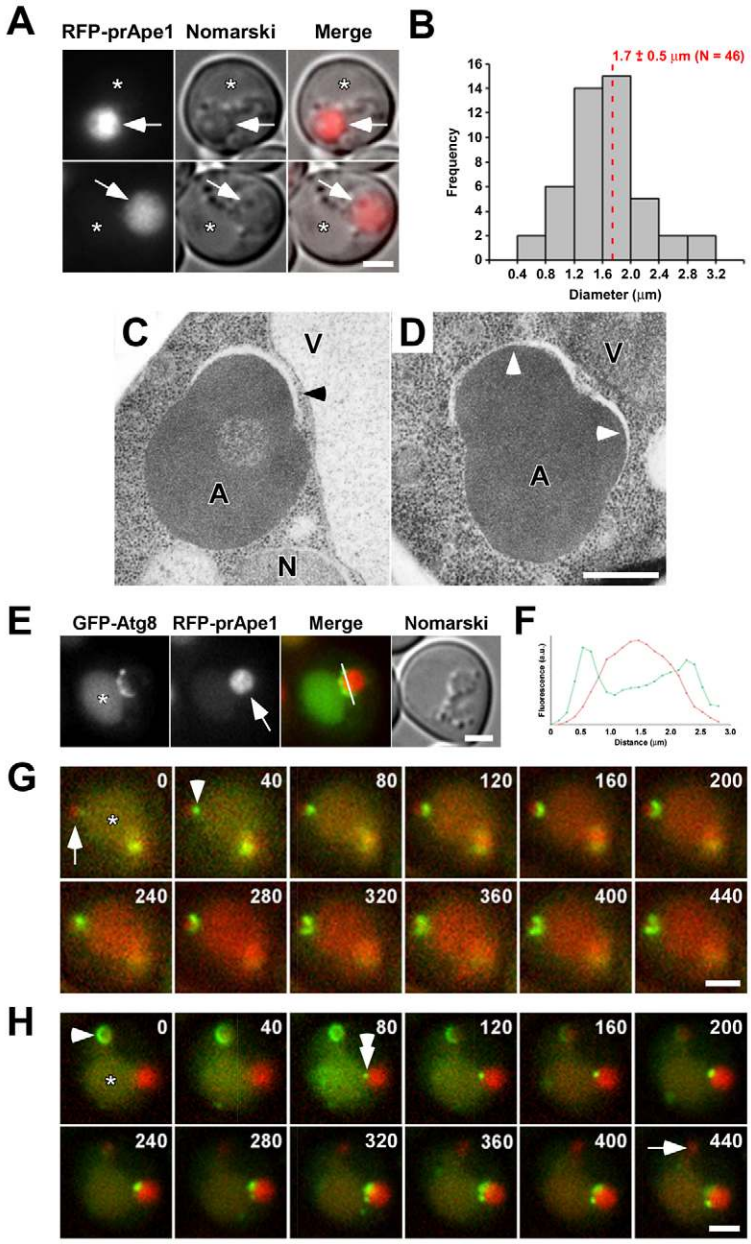

Fig. 1. GAC enables visualization of IMs. (**A**) Overexpression of prApe1 enables visualization of the Ape1 complex under a bright-field microscope with Nomarski optics. Wild-type cells expressing RFP–Ape1 at the natural expression level (GYS638) carrying pYEX-BX[prApe1] were grown in SDCA medium containing $CuSO_4$ and treated with rapamycin for 5 hours. Arrows indicate the GAC. Asterisks indicate vacuoles. Scale bar: 2 μm. (**B**) Histogram of the diameters of GACs outside the vacuole. Diameters were measured for cells in A using MetaMorph software. Red dotted line indicates the average diameter. Cells were treated with rapamycin for 5 hours. (**C**,**D**) Electron micrographs of a GAC. Wild-type cells overexpressing prApe1 were grown in SDCA medium containing $CuSO_4$ and treated with rapamycin for 5 hours. A, Ape1 complex; V, vacuole; N, nucleus. Arrowheads indicate membranous structures. Scale bar: 500 nm. (**E**) The GAC enables IM identification under the fluorescence microscope. Wild-type cells expressing RFP–Ape1 at a natural expression level and harboring pRS314[GFP-Atg8] and pYEX-BX[prApe1] were grown in SDCA medium containing $CuSO_4$ and treated with rapamycin for 6 hours. An asterisk and an arrow indicate the vacuole and the GAC, respectively. Scale bar: 2 μm. (**F**) Fluorescence profiles of GFP (green) and RFP (red) measured along the white line in E. (**G**,**H**) Time-lapse images of GFP–Atg8. Cells were treated with rapamycin for 2–3 hours before observation. Images were taken every 40 seconds. GFP–Atg8 and RFP–prApe1 are colored green and red, respectively. Arrows, GAC; arrowheads and double arrowhead, GFP–Atg8; asterisks, vacuoles. Scale bar: 2 μm.

CPY) to the vacuole (Raymond et al., 1992), Vps15, Vps30 and Vps34 are essential for autophagosome formation as components of phosphatidylinositol (PtdIns) 3-kinase complex I (Kametaka et al., 1998; Kihara et al., 2001; Obara et al., 2008a). We investigated the localization of representative GFP-fused Atg and Vps proteins in GAC cells expressing 2×mCherry–Atg8 (Ch–Atg8), and finely mapped the localization of Atg/Vps proteins during IM expansion. PAS scaffold proteins (Atg13 and Atg17) and PtdIns 3-kinase complex I were localized to a dot at the junction between the IM and the vacuolar membrane (arrowheads in Fig. 3), which we termed the vacuole-IM contact site (VICS). By contrast, Atg1, Atg8 and the Atg16–Atg12–Atg5 complex labeled the VICS and the IM (Fig. 3). We measured the fluorescence intensity along the IM and found that the profiles of these proteins and Ch–Atg8 overlapped extensively (Fig. 3). Thus, we designate this localization as the 'IM' pattern. The Atg2–Atg18 complex and Atg9 were distributed as two or three dots associated with the IM; some of these dots were apparently distinct from the VICS (Fig. 3). Time-lapse microscopy showed that Atg2–GFP was initially visualized as a dot and subsequently appeared as multiple dots at the edge of the IM (supplementary material Fig. S2). Thus, we designate this localization as the 'IM edge' pattern. These patterns correlate with known functional units, with several exceptions, as detailed in the following sections.

The localization of Atg1 is distinct from that of its regulators

Upon starvation, Atg1 and Atg13 interact with the Atg17–Atg29–Atg31 complex to form the Atg1–Atg13–Atg17–Atg29–Atg31 complex (hereafter, the PAS scaffold complex), in a manner independent of Atg1 kinase activity (Kabeya et al., 2009; Kamada et al., 2000; Kawamata et al., 2008). We used Atg13 and Atg17 as representative components of the PAS scaffold

complex; both proteins were localized to the VICS (Fig. 3), suggesting that Atg13 and Atg17 stay at the VICS during IM expansion. In contrast, Atg1 exhibited the IM pattern (Fig. 3), indicating that a substantial proportion of Atg1 dissociates from the PAS scaffold complex. Atg1 is, at least in part, localized to the inner surface of the IM, because Atg1 is enclosed in autophagosomes and subsequently delivered to the vacuole (Nakatogawa et al., 2012b).

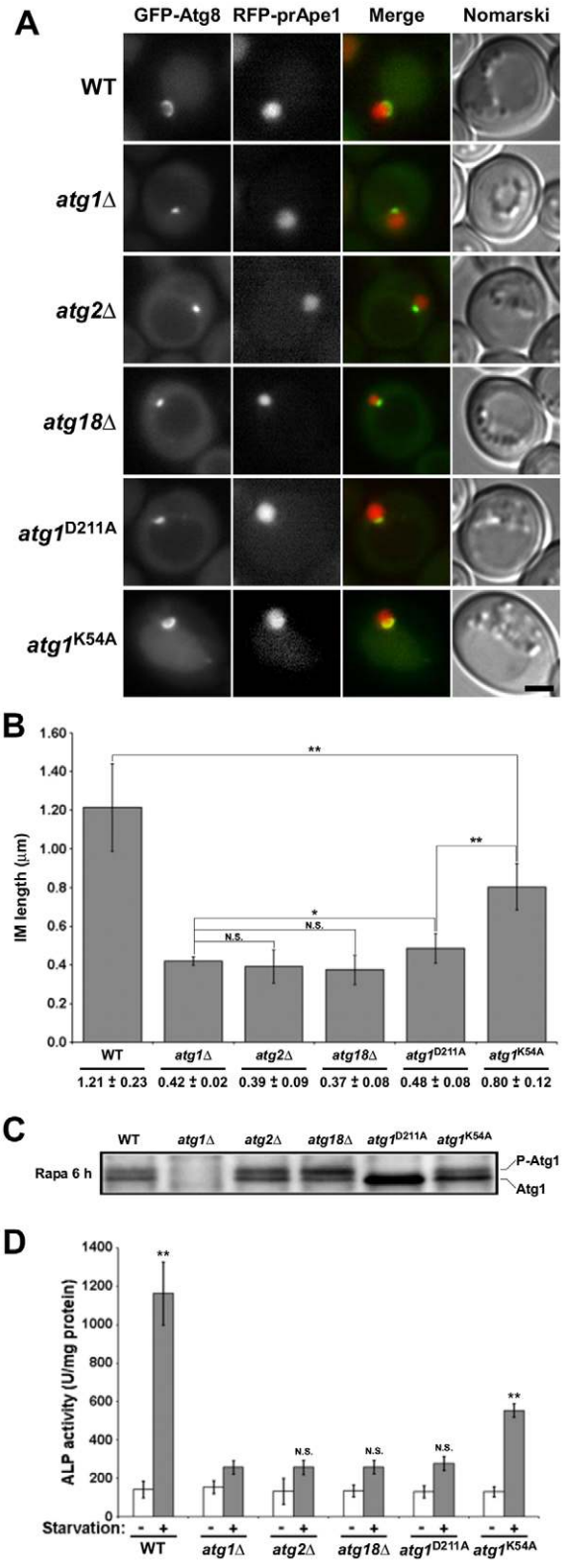

Fig. 2. Lengths of the IMs reflect the magnitude of autophagy. (**A**) RFP–prApe1-expressing cells harboring pRS314[GFP-ATG8] and pYEX-BX[prAPE1] were grown in SDCA medium containing $CuSO_4$ and treated with rapamycin for 6 hours. Scale bar: 2 μm. (**B**) Lengths of IMs, estimated from the images in A. Fluorescence intensities of GFP–Atg8 were measured using the 'linescan' function of the MetaMorph software, and FWHM (full width at half maximum) was calculated from each graph. Wild-type ($n=10$), *atg1*Δ ($n=8$), *atg2*Δ ($n=17$), *atg18*Δ ($n=19$), *atg1*^{D211A} ($n=12$) and *atg1*^{K54A} ($n=13$) cells were used. Error bars indicate standard deviations. *$P<0.05$; **$P<0.001$; N.S. (not significant) indicates $P>0.05$ (two-tailed Student's *t*-test). (**C**) Autophosphorylation of Atg1. Cells were grown in YEPD medium and incubated in the presence of rapamycin for 6 hours; cell lysates were prepared by the alkaline lysis method. Aliquots of cell lysates (0.05 OD_{600} units) were subjected to immunoblot analysis using an anti-Atg1 antiserum. The slower-migrating bands represent phosphorylated Atg1 (P-Atg1), and the faster-migrating bands represent unphosphorylated Atg1 (Atg1). (**D**) Activity of bulk autophagy, estimated by the alkaline phosphatase assay. Cells harboring pTN3 were grown in SDCA medium and transferred to SD(–N) medium. Collected cells were subjected to the alkaline phosphatase assay (Noda et al., 1995). **$P<0.001$; N.S. (not significant) indicates $P>0.05$ (two-tailed Student's *t*-test).

Phosphatidylinositol 3-kinase complex I stays at the VICS

In *S. cerevisiae*, two distinct PtdIns 3-kinase complexes have been identified: PtdIns 3-kinase complex I, which is required for autophagy and consists of Vps15, Vps34, Vps30 and Atg14; and PtdIns 3-kinase complex II, which is required for the VPS pathway and contains Vps38 instead of Atg14 (Kihara et al., 2001). We visualized Vps15–GFP, Vps30–GFP and Atg14–GFP and showed that PtdIns 3-kinase complex I was localized to the VICS during IM expansion (Fig. 3). In addition, we showed that dots labeled with Vps38–GFP did not associate with the IM (supplementary material Fig. S3), further indicating that PtdIns complex II is dispensable for autophagosome formation.

Previously, using GFP-2×FYVE as a probe, our group showed that phosphatidylinositol 3-phosphate [PtdIns(3)*P*], a product of the PtdIns 3-kinases, is localized to the IM (Obara et al., 2008a). The fact that the PtdIns 3-kinase complex I is localized to the VICS during IM expansion suggests that PtdIns(3)*P* is mainly produced at the VICS.

Atg16 and the Atg12–Atg5 conjugate exhibit the IM pattern

Localization analysis of Atg5–GFP and Atg16–GFP in GAC cells revealed that these proteins exhibited the IM pattern (Fig. 3). Thus, Atg5 and Atg16 are markers for the IM in *S. cerevisiae* as well as in mammalian cells (Mizushima et al., 2003; Mizushima et al., 2001). Association of Atg16 with Atg5 is important for targeting the Atg12–Atg5 conjugate to the PAS (Matsushita et al., 2007), suggesting that this interaction is required for their localization to the IM. Our group has reported that Atg12–Atg5 exerts an E3-like function in the conjugation of Atg8 with phosphatidylethanolamine (PE) to produce Atg8–PE (Hanada et al., 2007). IM localization of both the Atg12–Atg5 conjugate and Atg8 suggests that the Atg12–Atg5 conjugate continuously generates Atg8–PE on the IM. Because the Atg12–Atg5 conjugate does not label autophagosomes accumulated in the cytoplasm in *ypt7*Δ cells (Suzuki et al., 2001), the conjugate is not localized to either the outer or the inner membrane of mature

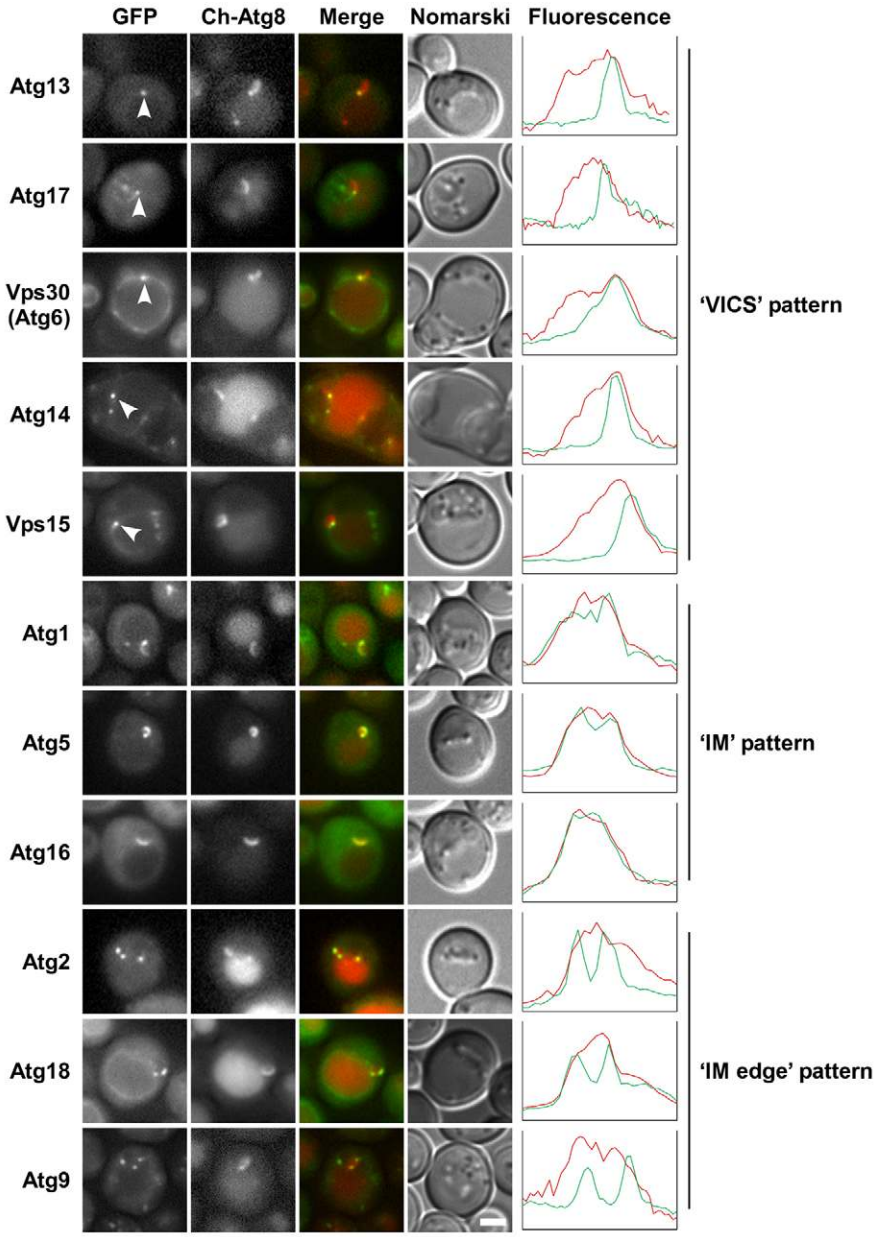

Fig. 3. Fine mapping of Atg proteins on the IMs. Cells expressing C-terminally GFP-fused Atg/Vps proteins were transformed with pRS314[2×mCherry-Atg8] and pYEX-BX[prApe1]. The cells were grown in SDCA medium containing $CuSO_4$ and treated with rapamycin. Fluorescence images of mCherry–Atg8 (Ch–Atg8) and GFP-fused Atg/Vps proteins (GFP) were merged (Merge). Fluorescence profiles along the IMs from the distal end to the vacuole are shown from left to right (Fluorescence). Based on these images, the localization of Atg/Vps proteins on IMs can be classified into three categories, as indicated. Arrowheads indicate the VICS. Scale bar: 2 μm.

autophagosomes. Instead, the conjugate might be localized solely to the outer surface of the IM, and dissociate when autophagosome formation is completed.

Atg2–Atg18 complex and Atg9 are localized to the edge of the IM

Atg2 and Atg18 form a complex and are localized to the PAS interdependently (Obara et al., 2008b; Suzuki et al., 2007). Because both Atg2 and Atg18 exhibited the IM edge pattern in GAC cells (Fig. 3), we examined the spatial relationship between Atg2 and Atg18, and confirmed that they were colocalized to multiple positions along the GAC (arrows in Fig. 4A), suggesting that they are localized to the IM edge as a complex. Atg18 is a phosphoinositide binding protein that preferentially binds to PtdIns(3)*P* and PtdIns(3,5)P_2 (Dove et al., 2004; Strømhaug et al., 2004). Our hierarchical analysis revealed that the PtdIns 3-kinase complex I is required for PAS localization of the Atg2–Atg18 complex (Suzuki et al., 2007). The fact that PtdIns 3-kinase complex I is absent from the IM (Fig. 3) suggests that the IM edge distribution of the Atg2–Atg18 complex is not dependent on the PtdIns 3-kinase complex I itself but instead on its product, PtdIns(3)*P*. Because PtdIns(3)*P* is distributed throughout the entire inner surface of the IM (Obara et al., 2008a), another mechanism may be required to restrict the localization of the Atg2–Atg18 complex to the IM edge.

Among the Atg proteins, Atg9 is the sole integral membrane protein essential for autophagosome formation (Noda et al., 2000). In GAC cells, Atg9 also exhibited the IM edge pattern (Fig. 3). Fluorescence microscopy showed that Atg9 was, at least in part, colocalized with the Atg2–Atg18 complex at the IM edge (Fig. 4B). Previous studies have shown that Atg2 and Atg18 physically interact with Atg9 (Reggiori et al., 2005; Wang et al., 2001). Therefore, Atg9 might interact with the Atg2–Atg18 complex at the IM edge. Our recent work has shown that Atg9

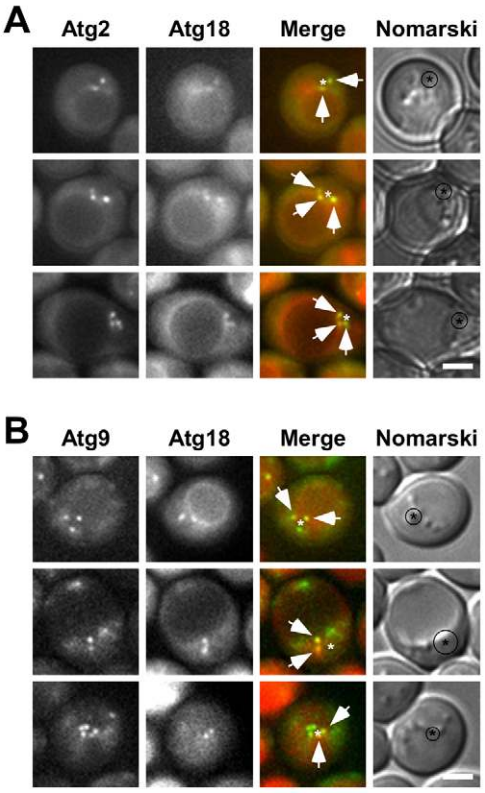

Fig. 4. The Atg2–Atg18 complex and Atg9 are colocalized at the edge of the IM. Cells were grown in SDCA medium containing $CuSO_4$ and treated with rapamycin for 3 hours. (**A**) Images of cells harboring pYEX-BX[prApe1] and chromosomally integrated Atg2-2×GFP and Atg18-3×mCherry. Arrows indicate colocalized dots. Asterisks indicate positions of the GAC. Scale bar: 2 μm. (**B**) Images of cells harboring pYEX-BX[prApe1] and chromosomally integrated Atg9-2×GFP and Atg18-3×mCherry. Arrows indicate colocalized dots. Asterisks indicate positions of the GAC. Scale bar: 2 μm.

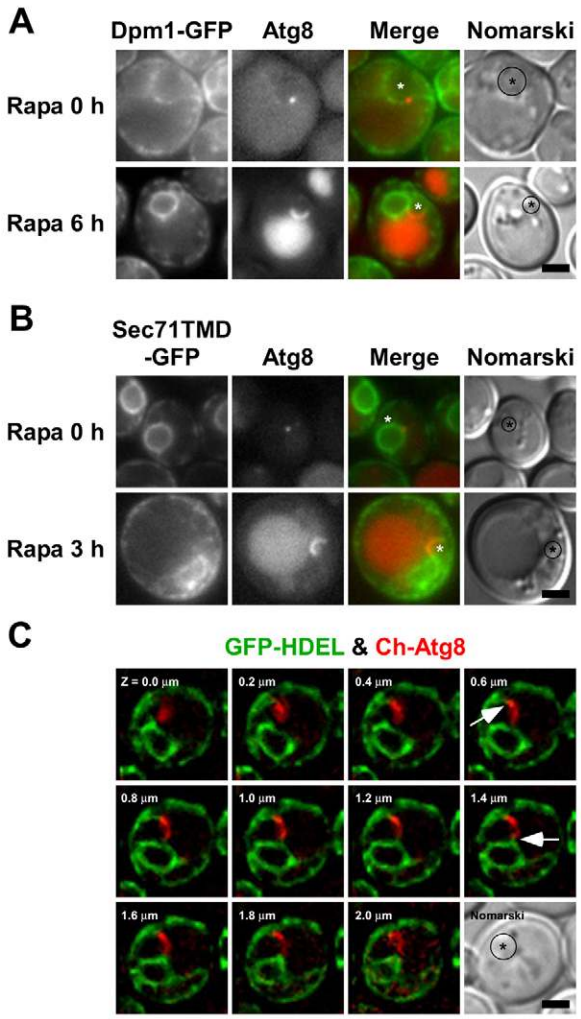

Fig. 5. ER is localized adjacent to the IM. Cells were grown in SDCA medium containing $CuSO_4$ and treated with rapamycin for the indicated number of hours. (**A**) Cells harboring pRS314[2×mCherry-Atg8] and pYEX-BX[prApe1] as well as chromosomally integrated Dpm1-GFP. Asterisks indicate positions of the GAC. Scale bar: 2 μm. (**B**) Cells chromosomally expressing Sec71TMD-GFP harboring pRS314[2×mCherry-Atg8] and pYEX-BX[prApe1]. Asterisks indicate positions of the GAC. Scale bar: 2 μm. (**C**) Three-dimensional images of cells harboring pMO13 (GFP-HDEL) and pRS424[P_{CUP1}-prApe1] as well as chromosomally integrated 2×mCherry-Atg8 (Ch-Atg8). An asterisk indicates the position of the GAC. Arrows indicate sites at which the IM and the ER are associated. Scale bar: 1 μm.

stays at the PAS during a cycle of autophagosome formation (Yamamoto et al., 2012); in conjunction with that data, we assume that Atg9 stays at the IM edge during one cycle of autophagosome formation.

Endoplasmic reticulum is localized adjacent to the IM

In mammalian cells, physical connections between IMs and the endoplasmic reticulum (ER) have been observed by electron microscopy (Hayashi-Nishino et al., 2009; Ylä-Anttila et al., 2009). We visualized the ER using Dpm1–GFP and Sec71TMD–GFP, which are ER transmembrane markers that exhibit a typical ER pattern, i.e. perinuclear and peripheral-network staining (Rossanese et al., 2001). We found that the IM was in close proximity to the ER (Fig. 5A,B). When we labeled the ER lumen with GFP–HDEL (his-asp-glu-leu) (Okamoto et al., 2006) and observed cells with three-dimensional fluorescence microscopy, we found that the IM was associated with the ER at two or three sites; the IM seemed to be connected with both the perinuclear and peripheral ER (arrows in Fig. 5C; supplementary material Fig. S4). Despite close association of IM with the ER, neither ER transmembrane nor lumenal proteins were ever detected at the IM (Fig. 5).

The IM is associated with ER exit sites

ER exit sites (ERES), which are subdomains of the ER specifically responsible for the production of COPII vesicles, can be labeled by fluorescent-protein-tagged Sec13 or Sec16 (Connerly et al., 2005). We visualized the localization of ERES in GAC cells by three-dimensional fluorescence microscopy, using Sec13–GFP as a marker, and found that the IM was located in close proximity to ERES at two or three sites per cell (Fig. 6A; supplementary material Fig. S5). The same result was obtained when Sec16–GFP was used (data not shown). Association of the IM with ERES labeled with Sec16–GFP was clearly detected in 79% of the cells (38 cells were examined three-dimensionally).

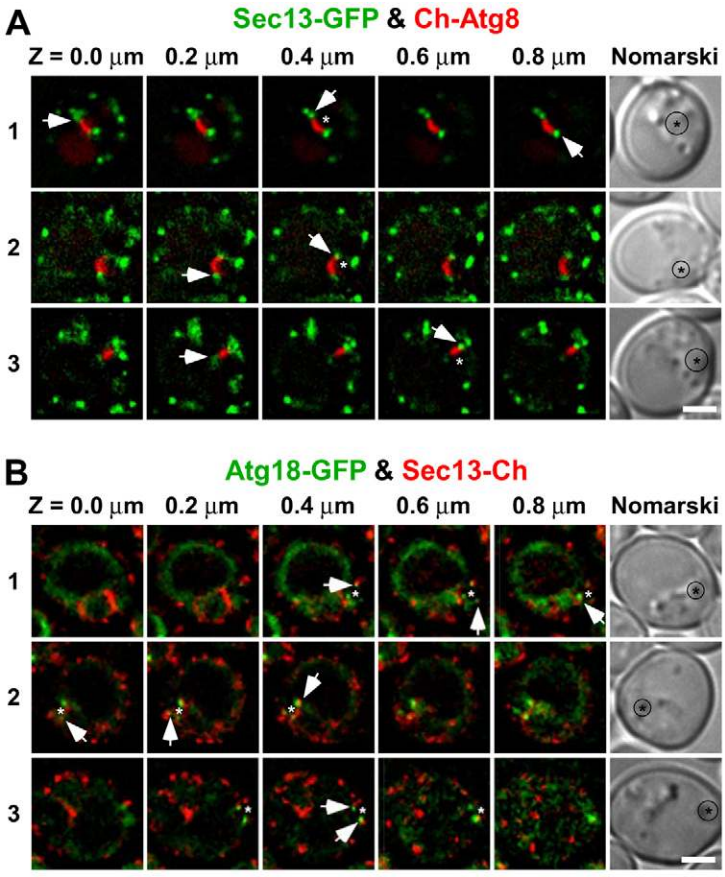

Fig. 6. The IM is associated with ERES. Cells were grown in SDCA medium containing $CuSO_4$ and treated with rapamycin. (**A**) Three sets of three-dimensional images of cells harboring pRS314[2×mCherry-Atg8] and pYEX-BX[prApe1] as well as chromosomally integrated Sec13-2×GFP. ERES labeled with Sec13 were localized in close proximity to the IM (arrows). Asterisks indicate positions of the GAC. Scale bar: 1 μm. (**B**) The Atg2–Atg18 complex is closely localized to ERES at the IM edge. Three sets of three-dimensional images of cells harboring pYEX-BX[prApe1] as well as chromosomally integrated Atg18-2×GFP and Sec13-2×mCherry (Sec13-Ch). ERES labeled with Sec13 were localized in close proximity to Atg18 at two or three sites per cell (arrows). Asterisks indicate positions of the GAC. Scale bar: 1 μm.

Sec16, which is essential for ER-to-Golgi transport, is thought to be involved in organization of ERES as a scaffold (Connerly et al., 2005). Previously, our group showed that a temperature-sensitive *sec16-2* mutant is defective in autophagy at the non-permissive temperature (Ishihara et al., 2001). These data suggest that ERES play important roles in IM expansion.

As mentioned above, IMs are associated with the ER at two or three sites per cell (Fig. 6A). We also show that the Atg2–Atg18 complex forms dots in two or three places at the edge of the IM (Fig. 3). These observations prompted us to examine the spatial relationship between ERES and the Atg2–Atg18 complex. By three-dimensional fluorescence microscopy, we found that dots labeled with Atg18 along the GAC were adjacent to ERES (Fig. 6B; supplementary material Fig. S6). Thus, the Atg2–Atg18 complex (and Atg9) might be involved in IM expansion by interacting with ERES at the IM edge.

Discussion

We have used the term PAS for a perivacuolar dot that most Atg proteins are localized to, and have called the dot detected in some *atg* disruptants the PAS, implying that the PAS is not accompanied by the IM. After the PAS is assembled, it acts to generate the IM. In *S. cerevisiae*, the IM has not been distinguishable from the PAS because of the resolution limit of light microscopy; thus in previous studies using wild-type cells, the PAS potentially included the IM.

In this study, taking advantage of the GAC cells, we visualized IMs by fluorescence microscopy and finely mapped the localizations of Atg proteins. We found that the PAS scaffold complex and PtdIns 3-kinase complex I were localized to the VICS. Atg1, Atg8 and the Atg16–Atg12–Atg5 complex labeled the VICS and the IM. We also found that the Atg2–Atg18 complex and Atg9 were localized to the IM edge but not to the VICS. Moreover, we showed that the IM is associated with the ER at the ERES; the Atg2–Atg18 complex and Atg9 may function at these junctions. Taken together, our data show that Atg proteins play individual roles at spatially distinct sites during IM expansion. These results will facilitate investigations of the function of each Atg protein in the near future.

Expansion of the IM

In wild-type GAC cells, the maximum length of the IM is 1.21 μm (Fig. 2B). From the surface area of the IM, we can estimate the maximum diameter of an autophagosome composed of the same amount of lipids as the IM. When the IM is regarded as a disc, the maximum length of the IM corresponds to the diameter. In this case, the area of the IM approximately equals the surface area of a sphere with a diameter of 0.61 μm (supplementary material Fig. S7). When the IM is regarded as a hemisphere, the area of the IM approximately equals the surface area of a sphere with a diameter of 0.86 μm (supplementary material Fig. S7). The diameter of an autophagic body, the inner membrane structure of an autophagosome, is ~0.4–0.9 μm (Takeshige et al., 1992). Therefore, we believe that an amount of lipid necessary to form a normal-sized autophagosome is present at the IM in GAC cells. In *atg1*^{K54A} cells, the IM length is ~0.80 μm (Fig. 2B). When the IM is regarded as a disc, the area of the IM approximately equals the surface area of a sphere with

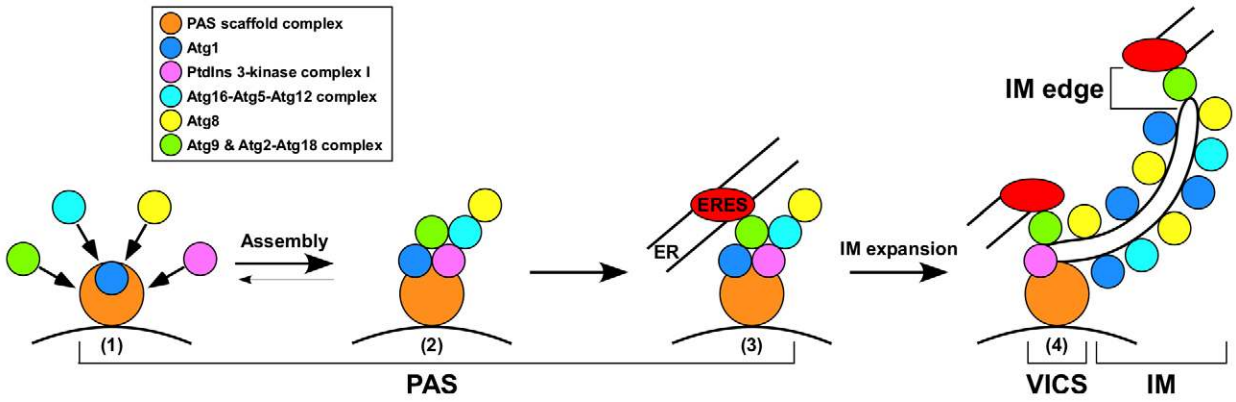

Fig. 7. Model for the mechanism of IM expansion. (1) Upon induction of autophagy, the PAS scaffold complex is assembled in an Atg1-kinase-activity-independent manner. (2) Subsequently, Atg proteins are assembled at the PAS; Atg9 might recruit lipids to the PAS. (3) IM formation is initiated; association of the PAS with ERES might trigger IM expansion. (4) The IM expands in an Atg1-kinase-activity-dependent manner. Atg proteins that exhibit the IM pattern transit to the IM. The Atg2–Atg18 complex and Atg9 might be involved in the association of the IM with ERES at the IM edge.

a diameter of 0.40 μm. When the IM is regarded as a hemisphere, the area of the IM approximately equals the surface area of a sphere with a diameter of 0.57 μm. Thus, the volume of an autophagosome in *atg1*^{K54A} cells is about 30% of that in wild-type cells. This value is consistent with the level of bulk autophagic activity of *atg1*^{K54A} cells (Fig. 2D).

GFP–Atg8 is targeted to the PAS in *atg1*Δ, *atg2*Δ and *atg18*Δ cells (Suzuki et al., 2007) but remains as an elliptical spot (Fig. 2A). This result indicates that both Atg1 and the Atg2–Atg18 complex are required for expansion of the IM. It has been reported that the Atg1 kinase activity is not necessary for PAS scaffold complex organization (Kabeya et al., 2005; Kamada et al., 2000). In this study, we dissected the contribution of Atg1 kinase activity to autophagosome formation, and found that IM length correlates with Atg1 kinase activity (Fig. 2). One explanation for these observations might be that the IM length is determined by a dynamic equilibrium. It is possible that a decrease in Atg1 kinase activity would shift this equilibrium towards a decrease in IM length. Identification of the substrate(s) of Atg1 will provide the means to definitively test this hypothesis.

The Atg2–Atg18 complex is the most downstream element in the hierarchy of PAS assembly (Suzuki et al., 2007); therefore, we postulated that this complex is involved in a later step of autophagosome formation, for example, the sealing of the IM. However, the data presented here clearly show that the Atg2–Atg18 complex is primarily required for IM expansion (Fig. 2A,B). It is still possible that the Atg2–Atg18 complex also functions at a later step of autophagosome formation.

Dynamics of the IM

Under starvation conditions, the fluorescence intensity of the GFP–Atg8 dot, which includes the PAS and the IM, next to the vacuole changes periodically. The period of each cycle is about 7–9 minutes; the intensity reaches a plateau within 4–5 minutes and then gradually decreases (Geng et al., 2008). This suggests that the formation of one autophagosome takes ~7–9 minutes in *S. cerevisiae*. Time-lapse microscopy of GAC cells revealed that the IM reaches its maximum length 5–6 minutes after its emergence (Fig. 1G), suggesting that the rate of IM expansion in GAC cells is comparable to that in wild-type cells.

Interestingly, paused IMs labeled with GFP–Atg8 disappear rapidly, within 2 minutes (Fig. 1H). Recently, our group has reported that Atg4 cleaves Atg8–PE exposed to the cytoplasm, and serves to provide a reservoir of free Atg8 (Nakatogawa et al., 2012a). Atg4 might be responsible for disintegrating paused IMs by cleaving Atg8–PE.

Fine mapping of Atg proteins during autophagosome formation

Based upon the results in this study, we propose a model for the mechanism of IM expansion (Fig. 7). Upon induction of autophagy, Atg1 and Atg13 interact with the Atg17–Atg29–Atg31 complex to form the PAS scaffold complex; this is a prerequisite step for assembly of downstream Atg proteins at the PAS (Kabeya et al., 2005; Kamada et al., 2000; Kawamata et al., 2008). Atg9 is an immediate downstream protein of Atg17 for PAS assembly (Suzuki et al., 2007). Since Atg9 exists on Atg9 vesicles (Yamamoto et al., 2012), Atg9 might provide lipids required for assembly of downstream proteins at the PAS. Subsequently, PtdIns 3-kinase complex I, which produces PtdIns(3)*P* at the PAS, is recruited to the PAS (Suzuki et al., 2007). Presumably, the primary role of PtdIns(3)*P* produced by complex I is recruitment of downstream Atg proteins, e.g. the Atg2–Atg18 complex and the products of two ubiquitin-like conjugation systems (the Atg16–Atg5–Atg12 complex and Atg8–PE) to the PAS.

During IM expansion, Atg proteins recruited to the PAS are distributed to distinct sites (Fig. 7). We showed that the PAS scaffold complex and the PtdIns 3-kinase complex I stay at the VICS (Fig. 3), supporting the notion that these proteins provide a platform for autophagosome formation. Please note that the Atg2–Atg18 complex and Atg9 are not localized to the VICS during IM expansion. Among the proteins in the PAS scaffold complex, only Atg1 is localized to the IM as well as the VICS. Atg1 kinase activity is essential for IM expansion (Fig. 2), suggesting that Atg1 phosphorylates target protein(s) at the VICS and the IM during IM expansion.

The activity of PtdIns 3-kinase complex I is necessary for autophagic pathways, possibly due to its role in recruitment of the Atg16–Atg5–Atg12 and Atg2–Atg18 complexes to the PAS (Suzuki et al., 2007). During autophagosome formation,

PtdIns(3)*P* is localized preferentially to the inner concave surface of the IMs, and it is subsequently enclosed in autophagosomes as a component of their inner membranes (Obara et al., 2008a). We show here that the PtdIns 3-kinase complex I is not localized to the IM (Fig. 3), suggesting that PtdIns(3)*P* is produced mainly at the VICS. PtdIns(3)*P* may play an important role by binding to an effector protein(s) at the inner surface of the IM, or it may be necessary to generate a negative membrane curvature at the inner surface of the IM.

The Atg16–Atg5–Atg12 complex, Atg8–PE and the Atg2–Atg18 complex act downstream in the PAS assembly pathway (Kawamata et al., 2008; Suzuki et al., 2007). All of these proteins are localized to the IM or the IM edge during autophagosome formation (Fig. 3). Because the Atg16–Atg5–Atg12 complex acts as an E3 enzyme in the generation of Atg8–PE (Hanada et al., 2007), its IM localization suggests that it catalyzes Atg8 lipidation on the IM.

Relationship between the Atg2–Atg18 complex and ERES

The Atg2–Atg18 complex is localized to the IM edge as multiple dots (Fig. 3; supplementary material Fig. S2). These dots are adjacent to ERES, which are subdomains specifically involved in COPII vesicle formation in the ER (Fig. 6B). These results suggest a tight relationship between the Atg2–Atg18 complex and ERES. Moreover, Atg9 is colocalized with the Atg2–Atg18 complex at the IM edge (Fig. 4B). Because ERES are involved in exit from the ER, the Atg2–Atg18 complex and Atg9 might play roles in entrance to the IM. Further functional analysis of the Atg2–Atg18 complex and Atg9 will improve our understanding of the mechanisms underlying IM expansion.

To date, the IM has been considered to be distinct from the endomembrane systems. In mammalian cells, physical connections of the IM with the ER have been reported (Hayashi-Nishino et al., 2009; Ylä-Anttila et al., 2009). Here, we show that the IM is associated with the ER at ERES. Our group has shown that the function of Sec16, which acts as a scaffold for ERES (Connerly et al., 2005; Yorimitsu and Sato, 2012), is important for autophagy (Ishihara et al., 2001). Sec13 is a coatomer of COPII vesicles, and is also used as a marker for ERES (Connerly et al., 2005). Recently, we have observed that knockdown of Sec13 results in a severe defect in autophagy (unpublished data). These results indicate that ERES play an important role in IM expansion.

Recently, a novel compartment for unconventional protein secretion of Acb1 (CUPS) has been reported (Bruns et al., 2011). Upon starvation, PtdIns(3)*P*, Grh1, Vps23, Atg8 and Atg9 are recruited to the one to three CUPS per cell. CUPS is localized near ERES labeled with Sec13 but separated from the ER. Although both CUPS and the IM are induced upon starvation, treatment with rapamycin alone is insufficient to form CUPS (Bruns et al., 2011). Moreover, Grh1–GFP, a CUPS marker, and Ape1–mCherry do not colocalize (Bruns et al., 2011). Autophagosome formation is completely inhibited in *atg11*Δ*atg17*Δ cells because of a defect in PAS assembly (Suzuki et al., 2007). In contrast, the relocalization of Grh1–GFP to CUPS is not impaired in *atg11*Δ*atg17*Δ cells (Bruns et al., 2011). These facts suggest that CUPS and the PAS/IM are distinct structures. Further morphological analysis by electron microscopy will provide new insights into these structures.

The absence of ER marker proteins from the IM indicates that these proteins do not transit to the IM from the ER (Fig. 5). There are two interpretations of this result. It may be that in yeast, the ER is associated with the IM in an indirect manner, possibly mediated by COPII vesicles. Alternatively, the ER and the IM of yeast might be directly connected, as has been demonstrated in mammalian cells (Hayashi-Nishino et al., 2009; Ylä-Anttila et al., 2009), but there are mechanisms that exclude ER proteins from the IM. Further studies will be required to clarify the role of the ER in IM expansion.

Materials and Methods

Yeast strains and growth conditions

The yeast strains used in this study are listed in supplementary material Table S1. Standard protocols were used for yeast manipulation (Adams et al., 1998). The mRFP–prApe1 strains were constructed as previously described (Strømhaug et al., 2004). Cells expressing C-terminally (1–2×)GFP- or (2–3×)mCherry-fused Atg/Vps proteins were generated using a PCR-based gene-modification method (Longtine et al., 1998). Cells chromosomally expressing Sec71TMD–GFP (YAM306) were generated by transforming wild-type cells with *Afl*II-digested fragments of the plasmid pRS305[SEC71TMD-GFP]. Cells were grown in synthetic defined plus casamino acid medium (SDCA; 0.17% yeast nitrogen base without amino acids and ammonium sulfate, 0.5% casamino acid, 0.5% ammonium sulfate and 2% glucose) with appropriate supplements. To drive the Cu^{2+}-inducible *CUP1* promoter, cells were cultured for 1 day in medium containing 250 μM $CuSO_4$ before use. Autophagy was induced by addition of 0.4 μg/ml rapamycin (Sigma) or by shifting to nitrogen starvation medium [SD(–N); 0.17% yeast nitrogen base without amino acids and ammonium sulfate and 2% glucose].

Plasmids

The plasmids used in this study are listed in supplementary material Table S2. pYEX-BX[prApe1] was generated by inserting the *Bgl*II cassette of *APE1* into pYEX-BX (Clontech) after digesting the plasmid with *Bam*HI. pRS424[P_{CUP1}-prApe1] was generated by inserting the blunted *Hin*dIII–*Sal*I fragment of *APE1* with the *CUP1* promoter excised from pYEX-BX[prApe1] into pRS424, after digesting the plasmid with *Pvu*II. pRS305[SEC71TMD-GFP] was generated by inserting the *Bam*HI–*Xho*I fragment of SEC71TMD-GFP from pRS306[SEC71TMD-GFP] (Sato et al., 2003) into pRS305, after digesting the plasmid with *Bam*HI and *Xho*I.

Fluorescence microscopy

Fluorescence microscopy was performed using an IX81 TIR-FM system (Olympus, Japan) equipped with a UPlanSApo 100× oil objective (NA: 1.40) and a CoolSNAP HQ CCD camera (Nippon Roper, Japan) as described previously (Suzuki et al., 2010). Blue (Sapphire 488-20, Coherent, USA) and yellow (85-YCA-010, Melles Griot, USA) lasers were used for excitation of GFP and mRFP/mCherry, respectively. Three-dimensional fluorescence images were acquired and processed using the MetaMorph software (Molecular Devices, USA).

Electron microscopy

Electron microscopy was performed by Tokai-EMA, Inc. (Nagoya, Japan) as described previously (Suzuki et al., 2011). Briefly, cells were harvested by centrifugation and media were removed by aspiration. The pellets were sandwiched with copper grids and rapidly frozen in liquid propane using Leica EM CPC (Leica, Germany). Cells were freeze-substituted in 2% osmium tetroxide dissolved in acetone. Samples were embedded in Quetol 651.

Immunoblot analysis

Cell lysates were prepared by the alkaline lysis method or by glass bead disruption (Horvath and Riezman, 1994; Suzuki et al., 2004). Primary antisera were anti-Atg1 (Matsuura et al., 1997) or anti-Ape1 (Suzuki et al., 2002). Horseradish-peroxidase-conjugated antibodies (Jackson ImmunoResearch, USA) were used as secondary antibodies. Chemiluminescence signals produced by an ECL reagent (PerkinElmer, Western Lightning Plus-ECL, USA; Wako, ImmunoStar LD, Japan) were detected using a CCD camera system (Fujifilm, LAS4000, Japan).

Acknowledgements

We thank Dr Ken Sato (Gunma University, Japan) and Dr Takehiko Yoko-o (National Institute of Advanced Industrial Science and Technology, Japan) for strains and plasmids, Dr Hitoshi Nakatogawa (Tokyo Institute of Technology, Japan) for comments on the manuscript, and Ms Mayumi Morimoto for technical assistance.

Author contributions

K.S. designed the project, worked on experiments using a fluorescence microscope and wrote the paper. M.A., C.K. and H.Y.

constructed plasmids and strains. H.Y. and Y.O. contributed to writing the paper. Y.O. supervised the entire project.

Funding

This work was supported by the Hamaguchi Foundation for the Advancement of Biochemistry [grant number H23-3 to K.S.]; the NOVARTIS Foundation (Japan) for the Promotion of Science [grant number 11-128 to K.S.]; and by Grants-in-Aids for Scientific Research from the Ministry of Education, Culture, Sports, Science and Technology of Japan [grant numbers 24121707, 24657083, 25291040 to K.S.; 24770182 to H.Y.; 23000015 to Y.O.]. Deposited in PMC for immediate release.

Supplementary material available online at
http://jcs.biologists.org/lookup/suppl/doi:10.1242/jcs.122960/-/DC1

References

Adams, A., Gottschling, D. E., Kaiser, C. A. and Stearns, T. (1998). *Methods in Yeast Genetics*. Cold Spring Harbor, NY: Cold Spring Harbor Laboratory Press.

Baba, M., Osumi, M., Scott, S. V., Klionsky, D. J. and Ohsumi, Y. (1997). Two distinct pathways for targeting proteins from the cytoplasm to the vacuole/lysosome. *J. Cell Biol.* **139**, 1687-1695.

Bruns, C., McCaffery, J. M., Curwin, A. J., Duran, J. M. and Malhotra, V. (2011). Biogenesis of a novel compartment for autophagosome-mediated unconventional protein secretion. *J. Cell Biol.* **195**, 979-992.

Connerly, P. L., Esaki, M., Montegna, E. A., Strongin, D. E., Levi, S., Soderholm, J. and Glick, B. S. (2005). Sec16 is a determinant of transitional ER organization. *Curr. Biol.* **15**, 1439-1447.

Dove, S. K., Piper, R. C., McEwen, R. K., Yu, J. W., King, M. C., Hughes, D. C., Thuring, J., Holmes, A. B., Cooke, F. T., Michell, R. H. et al. (2004). Svp1p defines a family of phosphatidylinositol 3,5-bisphosphate effectors. *EMBO J.* **23**, 1922-1933.

Geng, J., Baba, M., Nair, U. and Klionsky, D. J. (2008). Quantitative analysis of autophagy-related protein stoichiometry by fluorescence microscopy. *J. Cell Biol.* **182**, 129-140.

Hanada, T., Noda, N. N., Satomi, Y., Ichimura, Y., Fujioka, Y., Takao, T., Inagaki, F. and Ohsumi, Y. (2007). The Atg12-Atg5 conjugate has a novel E3-like activity for protein lipidation in autophagy. *J. Biol. Chem.* **282**, 37298-37302.

Hayashi-Nishino, M., Fujita, N., Noda, T., Yamaguchi, A., Yoshimori, T. and Yamamoto, A. (2009). A subdomain of the endoplasmic reticulum forms a cradle for autophagosome formation. *Nat. Cell Biol.* **11**, 1433-1437.

Horvath, A. and Riezman, H. (1994). Rapid protein extraction from *Saccharomyces cerevisiae*. *Yeast* **10**, 1305-1310.

Ishihara, N., Hamasaki, M., Yokota, S., Suzuki, K., Kamada, Y., Kihara, A., Yoshimori, T., Noda, T. and Ohsumi, Y. (2001). Autophagosome requires specific early Sec proteins for its formation and NSF/SNARE for vacuolar fusion. *Mol. Biol. Cell* **12**, 3690-3702.

Kabeya, Y., Kamada, Y., Baba, M., Takikawa, H., Sasaki, M. and Ohsumi, Y. (2005). Atg17 functions in cooperation with Atg1 and Atg13 in yeast autophagy. *Mol. Biol. Cell* **16**, 2544-2553.

Kabeya, Y., Noda, N. N., Fujioka, Y., Suzuki, K., Inagaki, F. and Ohsumi, Y. (2009). Characterization of the Atg17-Atg29-Atg31 complex specifically required for starvation-induced autophagy in *Saccharomyces cerevisiae*. *Biochem. Biophys. Res. Commun.* **389**, 612-615.

Kamada, Y., Funakoshi, T., Shintani, T., Nagano, K., Ohsumi, M. and Ohsumi, Y. (2000). Tor-mediated induction of autophagy via an Apg1 protein kinase complex. *J. Cell Biol.* **150**, 1507-1513.

Kamada, Y., Yoshino, K., Kondo, C., Kawamata, T., Oshiro, N., Yonezawa, K. and Ohsumi, Y. (2010). Tor directly controls the Atg1 kinase complex to regulate autophagy. *Mol. Cell. Biol.* **30**, 1049-1058.

Kametaka, S., Okano, T., Ohsumi, M. and Ohsumi, Y. (1998). Apg14p and Apg6/Vps30p form a protein complex essential for autophagy in the yeast, *Saccharomyces cerevisiae*. *J. Biol. Chem.* **273**, 22284-22291.

Kawamata, T., Kamada, Y., Kabeya, Y., Sekito, T. and Ohsumi, Y. (2008). Organization of the pre-autophagosomal structure responsible for autophagosome formation. *Mol. Biol. Cell* **19**, 2039-2050.

Kihara, A., Noda, T., Ishihara, N. and Ohsumi, Y. (2001). Two distinct Vps34 phosphatidylinositol 3-kinase complexes function in autophagy and carboxypeptidase Y sorting in *Saccharomyces cerevisiae*. *J. Cell Biol.* **152**, 519-530.

Kirisako, T., Baba, M., Ishihara, N., Miyazawa, K., Ohsumi, M., Yoshimori, T., Noda, T. and Ohsumi, Y. (1999). Formation process of autophagosome is traced with Apg8/Aut7p in yeast. *J. Cell Biol.* **147**, 435-446.

Klionsky, D. J., Cueva, R. and Yaver, D. S. (1992). Aminopeptidase I of *Saccharomyces cerevisiae* is localized to the vacuole independent of the secretory pathway. *J. Cell Biol.* **119**, 287-299.

Longtine, M. S., McKenzie, A., 3rd, Demarini, D. J., Shah, N. G., Wach, A., Brachat, A., Philippsen, P. and Pringle, J. R. (1998). Additional modules for versatile and economical PCR-based gene deletion and modification in *Saccharomyces cerevisiae*. *Yeast* **14**, 953-961.

Lynch-Day, M. A. and Klionsky, D. J. (2010). The Cvt pathway as a model for selective autophagy. *FEBS Lett.* **584**, 1359-1366.

Matsushita, M., Suzuki, N. N., Obara, K., Fujioka, Y., Ohsumi, Y. and Inagaki, F. (2007). Structure of Atg5·Atg16, a complex essential for autophagy. *J. Biol. Chem.* **282**, 6763-6772.

Matsuura, A., Tsukada, M., Wada, Y. and Ohsumi, Y. (1997). Apg1p, a novel protein kinase required for the autophagic process in *Saccharomyces cerevisiae*. *Gene* **192**, 245-250.

Mizushima, N., Yamamoto, A., Hatano, M., Kobayashi, Y., Kabeya, Y., Suzuki, K., Tokuhisa, T., Ohsumi, Y. and Yoshimori, T. (2001). Dissection of autophagosome formation using Apg5-deficient mouse embryonic stem cells. *J. Cell Biol.* **152**, 657-668.

Mizushima, N., Kuma, A., Kobayashi, Y., Yamamoto, A., Matsubae, M., Takao, T., Natsume, T., Ohsumi, Y. and Yoshimori, T. (2003). Mouse Apg16L, a novel WD-repeat protein, targets to the autophagic isolation membrane with the Apg12-Apg5 conjugate. *J. Cell Sci.* **116**, 1679-1688.

Mizushima, N., Yoshimori, T. and Ohsumi, Y. (2011). The role of Atg proteins in autophagosome formation. *Annu. Rev. Cell Dev. Biol.* **27**, 107-132.

Nakatogawa, H., Suzuki, K., Kamada, Y. and Ohsumi, Y. (2009). Dynamics and diversity in autophagy mechanisms: lessons from yeast. *Nat. Rev. Mol. Cell Biol.* **10**, 458-467.

Nakatogawa, H., Ishii, J., Asai, E. and Ohsumi, Y. (2012a). Atg4 recycles inappropriately lipidated Atg8 to promote autophagosome biogenesis. *Autophagy* **8**, 177-186.

Nakatogawa, H., Ohbayashi, S., Sakoh-Nakatogawa, M., Kakuta, S., Suzuki, S. W., Kirisako, H., Kondo-Kakuta, C., Noda, N. N., Yamamoto, H. and Ohsumi, Y. (2012b). The autophagy-related protein kinase Atg1 interacts with the ubiquitin-like protein Atg8 via the Atg8 family interacting motif to facilitate autophagosome formation. *J. Biol. Chem.* **287**, 28503-28507.

Noda, T., Matsuura, A., Wada, Y. and Ohsumi, Y. (1995). Novel system for monitoring autophagy in the yeast *Saccharomyces cerevisiae*. *Biochem. Biophys. Res. Commun.* **210**, 126-132.

Noda, T., Kim, J., Huang, W. P., Baba, M., Tokunaga, C., Ohsumi, Y. and Klionsky, D. J. (2000). Apg9p/Cvt7p is an integral membrane protein required for transport vesicle formation in the Cvt and autophagy pathways. *J. Cell Biol.* **148**, 465-480.

Obara, K., Noda, T., Niimi, K. and Ohsumi, Y. (2008a). Transport of phosphatidylinositol 3-phosphate into the vacuole via autophagic membranes in *Saccharomyces cerevisiae*. *Genes Cells* **13**, 537-547.

Obara, K., Sekito, T., Niimi, K. and Ohsumi, Y. (2008b). The Atg18-Atg2 complex is recruited to autophagic membranes via phosphatidylinositol 3-phosphate and exerts an essential function. *J. Biol. Chem.* **283**, 23972-23980.

Okamoto, M., Yoko-o, T., Umemura, M., Nakayama, K. and Jigami, Y. (2006). Glycosylphosphatidylinositol-anchored proteins are required for the transport of detergent-resistant microdomain-associated membrane proteins Tat2p and Fur4p. *J. Biol. Chem.* **281**, 4013-4023.

Raymond, C. K., Howald-Stevenson, I., Vater, C. A. and Stevens, T. H. (1992). Morphological classification of the yeast vacuolar protein sorting mutants: evidence for a prevacuolar compartment in class E vps mutants. *Mol. Biol. Cell* **3**, 1389-1402.

Reggiori, F., Shintani, T., Nair, U. and Klionsky, D. J. (2005). Atg9 cycles between mitochondria and the pre-autophagosomal structure in yeasts. *Autophagy* **1**, 101-109.

Robinson, J. S., Klionsky, D. J., Banta, L. M. and Emr, S. D. (1988). Protein sorting in *Saccharomyces cerevisiae*: isolation of mutants defective in the delivery and processing of multiple vacuolar hydrolases. *Mol. Cell. Biol.* **8**, 4936-4948.

Rossanese, O. W., Reinke, C. A., Bevis, B. J., Hammond, A. T., Sears, I. B., O'Connor, J. and Glick, B. S. (2001). A role for actin, Cdc1p, and Myo2p in the inheritance of late Golgi elements in *Saccharomyces cerevisiae*. *J. Cell Biol.* **153**, 47-62.

Sato, K., Sato, M. and Nakano, A. (2003). Rer1p, a retrieval receptor for ER membrane proteins, recognizes transmembrane domains in multiple modes. *Mol. Biol. Cell* **14**, 3605-3616.

Shintani, T. and Klionsky, D. J. (2004). Cargo proteins facilitate the formation of transport vesicles in the cytoplasm to vacuole targeting pathway. *J. Biol. Chem.* **279**, 29889-29894.

Shintani, T., Huang, W. P., Stromhaug, P. E. and Klionsky, D. J. (2002). Mechanism of cargo selection in the cytoplasm to vacuole targeting pathway. *Dev. Cell* **3**, 825-837.

Sikorski, R. S. and Hieter, P. (1989). A system of shuttle vectors and yeast host strains designed for efficient manipulation of DNA in *Saccharomyces cerevisiae*. *Genetics* **122**, 19-27.

Stephan, J. S., Yeh, Y. Y., Ramachandran, V., Deminoff, S. J. and Herman, P. K. (2009). The Tor and PKA signaling pathways independently target the Atg1/Atg13 protein kinase complex to control autophagy. *Proc. Natl. Acad. Sci. USA* **106**, 17049-17054.

Strømhaug, P. E., Reggiori, F., Guan, J., Wang, C. W. and Klionsky, D. J. (2004). Atg21 is a phosphoinositide binding protein required for efficient lipidation and localization of Atg8 during uptake of aminopeptidase I by selective autophagy. *Mol. Biol. Cell* **15**, 3553-3566.

Suzuki, K., Kirisako, T., Kamada, Y., Mizushima, N., Noda, T. and Ohsumi, Y. (2001). The pre-autophagosomal structure organized by concerted functions of *APG* genes is essential for autophagosome formation. *EMBO J.* **20**, 5971-5981.

Suzuki, K., Kamada, Y. and Ohsumi, Y. (2002). Studies of cargo delivery to the vacuole mediated by autophagosomes in *Saccharomyces cerevisiae*. *Dev. Cell* **3**, 815-824.

Suzuki, K., Noda, T. and Ohsumi, Y. (2004). Interrelationships among Atg proteins during autophagy in *Saccharomyces cerevisiae*. *Yeast* **21**, 1057-1065.
Suzuki, K., Kubota, Y., Sekito, T. and Ohsumi, Y. (2007). Hierarchy of Atg proteins in pre-autophagosomal structure organization. *Genes Cells* **12**, 209-218.
Suzuki, K., Kondo, C., Morimoto, M. and Ohsumi, Y. (2010). Selective transport of α-mannosidase by autophagic pathways: identification of a novel receptor, Atg34p. *J. Biol. Chem.* **285**, 30019-30025.
Suzuki, K., Morimoto, M., Kondo, C. and Ohsumi, Y. (2011). Selective autophagy regulates insertional mutagenesis by the Ty1 retrotransposon in *Saccharomyces cerevisiae*. *Dev. Cell* **21**, 358-365.
Takeshige, K., Baba, M., Tsuboi, S., Noda, T. and Ohsumi, Y. (1992). Autophagy in yeast demonstrated with proteinase-deficient mutants and conditions for its induction. *J. Cell Biol.* **119**, 301-311.
Wang, C. W., Kim, J., Huang, W. P., Abeliovich, H., Stromhaug, P. E., Dunn, W. A., Jr and Klionsky, D. J. (2001). Apg2 is a novel protein required for the cytoplasm to vacuole targeting, autophagy, and pexophagy pathways. *J. Biol. Chem.* **276**, 30442-30451.
Xie, Z. and Klionsky, D. J. (2007). Autophagosome formation: core machinery and adaptations. *Nat. Cell Biol.* **9**, 1102-1109.
Yamamoto, H., Kakuta, S., Watanabe, T. M., Kitamura, A., Sekito, T., Kondo-Kakuta, C., Ichikawa, R., Kinjo, M. and Ohsumi, Y. (2012). Atg9 vesicles are an important membrane source during early steps of autophagosome formation. *J. Cell Biol.* **198**, 219-233.
Ylä-Anttila, P., Vihinen, H., Jokitalo, E. and Eskelinen, E. L. (2009). 3D tomography reveals connections between the phagophore and endoplasmic reticulum. *Autophagy* **5**, 1180-1185.
Yorimitsu, T. and Sato, K. (2012). Insights into structural and regulatory roles of Sec16 in COPII vesicle formation at ER exit sites. *Mol. Biol. Cell* **23**, 2930-2942.